PHILOSOPHICAL TRANSACTIONS OF THE ROYAL SOCIETY A MATHEMATICAL, PHYSICAL & ENGINEERING SCIENCES

Cubic Phases of Self-Assembled Amphiphilic Aggregates

John M. Seddon and Richard H. Templer

Phil. Trans. R. Soc. Lond. A 1993 **344**, 377-401
doi: 10.1098/rsta.1993.0096

Cubic phases of self-assembled amphiphilic aggregates

By John M. Seddon and Richard H. Templer

Department of Chemistry, Imperial College of Science, Technology and Medicine, Exhibition Road, London SW7 2AY, U.K.

In this paper we give an overview of cubic liquid-crystalline mesophases formed by amphiphiles. In §1 we present brief descriptions of the principal types of translationally ordered lyotropic phases, and describe the locations in the phase diagrams where the different types of cubic phase occur. In §2 we discuss the various forces that act between bilayers. These transverse interactions are relatively straightforward to quantify in the case of lamellar phases, but are more complex for cubic phases, because of the non-planar geometry. In §3 we show how an intrinsic desire for interfacial curvature can lead to a state of physical frustration. We then introduce the curvature elastic energy, and describe how this may be related to the stress profile across the bilayer. In the following sections we focus attention on the *inverse* (water-in-oil) versions of the non-lamellar phases, although analogous effects also operate in the normal topology (oil-in-water) structures. In §4 we briefly describe the inverse hexagonal phase, which is the simplest inverse phase with curved interfaces. This allows us to illustrate the role of hydrocarbon chain packing frustration in a rather clear way before coming on to the more subtle interplay between packing and curvature frustration, characteristic of the bicontinuous cubic phases, which is discussed in §5. In §6 we describe an entirely different class of cubic phases, with positive interfacial gaussian curvature. These cubic phases are composed of complex packings of discrete micellar or inverse micellar aggregates, which may be quasi-spherical and/or anisotropic in shape. Finally, in §7 we discuss geometric aspects of transitions between lamellar, hexagonal and cubic phases, and show how determination of the epitaxial relations between phases can shed light on the precise mechanisms of the phase transitions.

1. Introduction

This paper is concerned with the extraordinarily rich lyotropic liquid-crystalline phase behaviour of amphiphilic molecules. We will only consider translationally ordered phases, i.e. we will say nothing about micellar solutions, microemulsions or sponge phases, which are described elsewhere in this Issue. Furthermore, at low temperature and/or hydration, amphiphiles tend to adopt various structures such as the gel phases, in which the hydrocarbon chain conformation is partially ordered or even fully crystalline; these structures will also not be discussed here. Although we will briefly mention the simpler lamellar and hexagonal phases, our main focus here is on the lyotropic cubic phases, which are extraordinary liquid-crystalline structures with three-dimensional periodicity.

A typical example of a class of amphiphilic molecules is the phospholipids, which form the basic fluid bilayer structure of the biomembranes of all living cells. If we

Phil. Trans. R. Soc. Lond. A (1993) **344**, 377–401
Printed in Great Britain

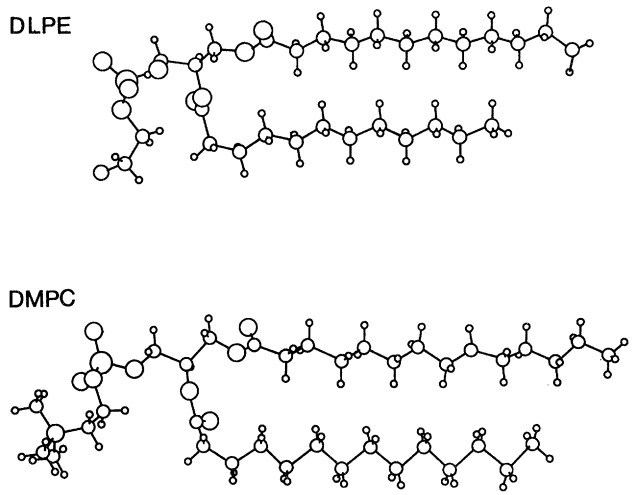

Figure 1. Molecular conformations of DLPE and DMPC in the crystalline lamellar phase. Adapted from Pascher *et al.* (1992).

compare the single crystal structures of dilauroylphosphatidylethanolamine (DLPE) and dimyristoylphosphatidylcholine (DMPC) (Pascher *et al.* 1992), examples of the two most common types of phospholipid found in animal cell membranes, we see that the molecular conformations are in fact rather similar (figure 1). However, the lyotropic phase behaviour of these two classes of lipid is dramatically different (Seddon 1990*a*), due to the difference in the headgroup-headgroup and headgroup-water interactions (such as hydrogen-bonding) induced by replacement of the PC terminal trimethylammonium group with a simple ammonium group in PE. Thus a seemingly rather minor chemical modification can have drastic consequences for the lyotropic phase behaviour. A vast literature exists, documenting the effect of various factors such as temperature, hydration, chainlength, headgroup modification, pH, salt concentration, and the presence of polar, non-polar or amphiphilic solutes. A number of review articles may be consulted for further details of these aspects (Luzzati 1968; Shipley 1973; Charvolin & Tardieu 1978; Tiddy 1980; Small 1986; Larsson 1989; Lindblom & Rilfors 1989; Gruner 1989; Fontell 1990; Seddon 1990*a*; Tate *et al.* 1991; Cevc & Marsh 1987). It is clear that an understanding of the precise form of the phase behaviour for a particular amphiphile would require a detailed consideration of many complex interactions, which are rather delicately balanced, and that this lies beyond our present understanding of these systems. Our aim here is to give a rather general overview of this area, stressing the underlying physical chemistry, rather than the fine details. The treatment and emphasis that we present here represents our own personal, idiosyncratic views of this complex and rapidly developing field.

In figure 2 we present a simple taxonomy of the major lyotropic liquid crystalline phases. We have arranged the ordering of the phases in this figure such that the lamellar L_α phase, which has a flat interface, occupies the central position and on either side of it the interfacial mean curvature of successive phases is steadily increasing in magnitude. To the left the interfacial curvature is towards the water, and by convention we describe this as negative mean curvature. Phases with negative mean interfacial curvature are known as type II, or inverse. Such phases are commonly formed by double-chain amphiphiles such as phospholipids. Conversely,

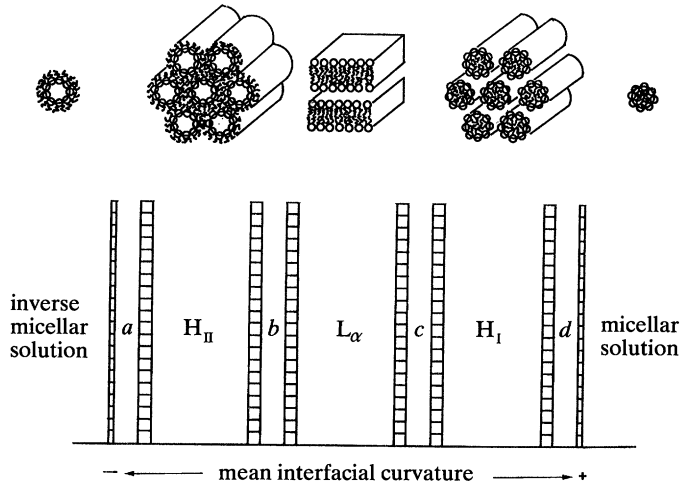

Figure 2. A taxonomy of the principal lyotropic liquid crystalline phases, arranged according to the mean curvature at the polar/non-polar interface.

to the right of the lamellar phase the curvature is increasingly away from the water, i.e. the curvature is positive. These phases are known as type I or normal phases. Such phases are typically formed by single-chain amphiphiles (detergents, surfactants, lysophospholipids, etc.). We will be more concerned with the inverse phases here, since they are of greater relevance to understanding membrane lipids.

The sequence of phases shown in figure 2 is often thought of as the *natural* sequence of the translationally ordered lyotropic mesophases. In this context one would imagine the water content increasing from left to right and thereby controlling the mean interfacial curvature. However, experimental phase diagrams never exhibit the entire sequence shown here and as we shall see real phase diagrams are sometimes out of this natural sequence. It should also be noted that many lyotropic phases can also form in various non-aqueous solvents such as glycerol, formamide or ethylammonium nitrate; there is thus nothing unique about water in this respect.

The lamellar L_α phase is the simplest and best understood of all of the lyotropic mesophases, consisting of a one dimensional stacking of amphiphilic bilayers (see figure 2). The simplest examples of mesophases with curved interfaces are the hexagonal H_I and H_{II} phases. Both of these structures are based on two dimensional, hexagonal packings of rods. For the H_I phase the rods are amphiphilic, whereas for the H_{II} phase they are polar, containing water cores surrounded by the polar headgroups of the amphiphile. In the H_I phase the aqueous continuum is a true solvent, in the sense that it can freely fill all of the available volume not occupied by the polar headgroups. On the other hand, the oil continuum of the H_{II} phase consists of fluid hydrocarbon chains which are tethered to the interfacial region, with energetically preferred conformational states. The thickness of the hydrocarbon region is thus quite severely constrained, and in any event cannot exceed a value set by the length of the fully extended chains (in the absence of added oil).

Experimentally it is of course vital to ascertain whether a phase is type I or type II. However, it is usually difficult (due to Babinet's principle) to distinguish the two types directly from their diffraction patterns (Luzzati 1968). A variety of methods may be used to obtain this information; the simplest is to note that usually a type I phase will eventually transform upon water dilution to a micellar solution,

PHILOSOPHICAL TRANSACTIONS OF THE ROYAL SOCIETY A MATHEMATICAL, PHYSICAL & ENGINEERING SCIENCES

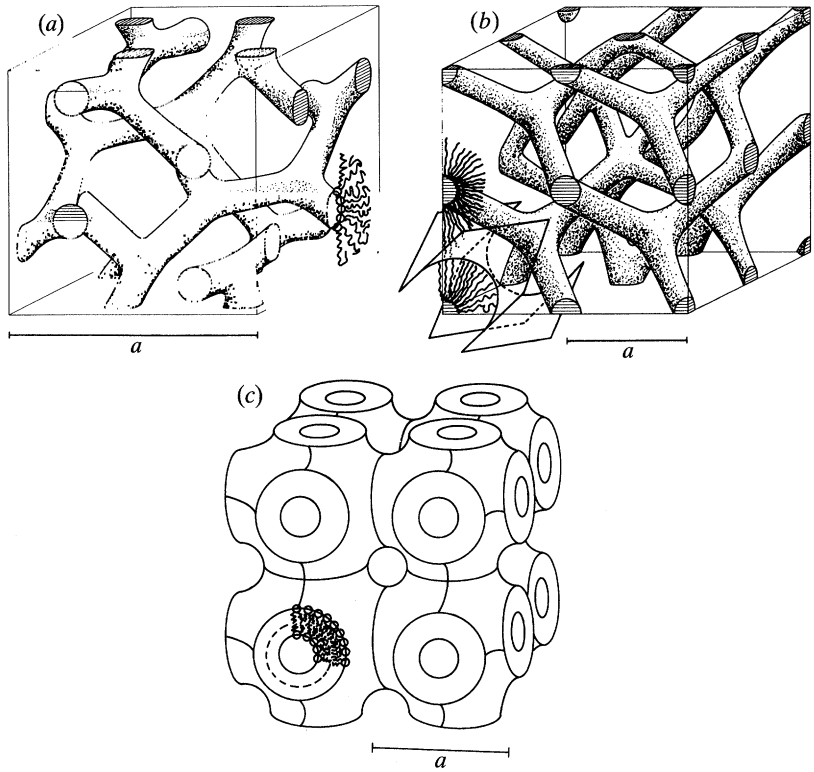

Figure 3. The structures of the well established inverse bicontinuous cubic phases. (*a*) The gyroid cubic phase, space group Ia3d (no. 230). (*b*) The double diamond cubic phase, space group Pn3m (no. 224), (*c*) The 'plumber's nightmare' cubic phase, space group Im3m (no. 229). Taken with permission from Seddon (1990).

whereas type II phases are frequently stable in the presence of a large excess water phase.

In addition to the relatively simple L_α, H_I and H_{II} phases, there are four further regions, marked *a*, *b*, *c* and *d* in figure 2, where more complex, translationally ordered phase structures may occur. These phases may be two dimensional or three dimensional, and many of the latter have cubic symmetry. In what follows we will concentrate on these cubic phases, although it should be remembered that other phase types also exist.

The cubic phases in regions *b* and *c* are now accepted to have the rather bizarre sponge-like structures shown in figure 3. The inverse cubic phases (region *b*) shown in the figure consist of a single continuous bilayer which divides space into two interwoven, congruent aqueous sub-volumes. The cubic phase is therefore said to be bicontinuous. The three inverse bicontinuous cubic phases of figure 3 are of crystallographic space groups Pn3m (no. 224), Im3m (no. 229) and Ia3d (no. 230). In the type I cubic phases the bilayer of figure 3 is replaced by water and the aqueous volumes are replaced by amphiphilic rods.

The most highly curved lyotropic liquid crystalline phases appear to be discontinuous cubic phases, consisting of packings of discrete inverse micellar, or micellar aggregates onto rather complex cubic lattices. These phases occur adjacent to the inverse micellar and normal micellar solutions, respectively, and are quite

distinct from the bicontinuous structures. It should be noted that various other examples of cubic phases have been reported, whose categorization according to the above scheme is to date uncertain.

We have too little space here to address the fascinating question as to the extent to which Nature has taken advantage of the rich liquid-crystalline behaviour of amphiphilic lipids to create ordered yet fluid biomembrane structures, and to modulate dynamic processes in cells. It is well known that the L_α phase forms the basis of the fluid bilayer structure of the cellular and intracellular membranes of all living organisms. The synthesis and maintenance of a flexible, fluid, self-healing permeability barrier only two molecules (approximately 40 Å) thick is enormously simplified by the self-assembly properties of amphiphilic membrane lipids. Furthermore, dynamic processes such as membrane fusion may be facilitated by the presence of lipids that have a preference for adopting the non-lamellar phases we have just described. Indeed, such lipids are extremely abundant in cell membranes, especially those that are biologically active. There is a very striking similarity between a fusion channel between two membranes, and the local structure of a bicontinuous cubic phase; indeed transformation of an L_α phase to such a cubic phase must occur via fusion events. A more subtle point is that the distribution of lateral stresses at different depths across a lipid bilayer, which affects its tendency to adopt non-lamellar phases (see §3), might play a regulatory role upon any embedded molecules such as membrane proteins. In this way the system might sense how close it was to a transition to a non-lamellar 'phase'. There is now quite convincing evidence that micro-organisms control the lipid composition of their membranes so as to maintain them close (but not too close) to a composition where non-lamellar structures would begin to appear. Bouligand (1990) has discussed a number of possible biological aspects of minimal surfaces and cubic phases. In particular he has suggested that because of geometrical packing considerations the presence of certain proteins embedded in the bilayer could induce the saddle deformations seen in the bicontinuous cubic phases, and that this may be responsible for some of the complex geometries and topologies adopted by various intra-cellular organelles. We will return to this point in §5.

2. Forces between bilayers

The lamellar L_α phase is the simplest of the phases to analyse, and serves as a useful starting point for understanding the structure and transverse interactions within the more complex lyotropic cubic phases. The equilibrium water layer thickness d_w is set primarily by a balance between the various interactions acting transverse to the layers (Cevc & Marsh 1987; Rand & Parsegian 1989; Israelachvili 1991). These consist both of attractive (van der Waals) and repulsive (hydrational/electrostatic/fluctuation, etc.) forces.

The simplest (non-retarded) form of the van der Waals attractive pressure (transverse force per unit area) between bilayers, valid for $d_w < 30$ Å, is

$$P_v = -H_A/6\pi d_w^3, \tag{2.1}$$

where the Hamaker constant H_A has a value of roughly 7×10^{-21} J for fluid phase phosphatidylcholine bilayers (for comparison, $kT = 4 \times 10^{-21}$ J at $T = 290$ K). The Hamaker constant decreases as d_w increases, due to retardation effects, and is also reduced in the presence of salts, due to ionic screening of the zero frequency

contribution to H_A. A more complete (although still non-retarded) form of the van der Walls interaction for a multibilayer stack is

$$P_v = \frac{-H_A}{6\pi d_w^3}\left[1 - \frac{2}{(1+d_{hc}/d_w)^3} + \frac{1}{(1+2d_{hc}/d_w)^3}\right] \tag{2.2}$$

where d_{hc} is the thickness of the hydrocarbon chain region of the bilayer.

The precise nature of the 'hydration force', which has a range of a few solvent molecule diameters, is still a matter of considerable controversy. However, it is generally of the form

$$P_h = P_0 \, e^{-d_w/\lambda}, \tag{2.3}$$

where for phospholipids P_0 is typically in the region of 8×10^8 N m^{-2}, and the decay length $\lambda = 1$–3 Å. At separations below 10–15 Å additional steric repulsions (peristaltic, protrusion and/or headgroup overlap) may come into effect (Israelachvili & Wennerström 1992).

For a simple lamellar phase of flexible bilayers, the pure fluctuation force arising from steric hindrance between adjacent layers, due to thermally excited layer undulations, has the Helfrich (1978) form

$$P_f = 3(\pi kT)^2/64 \, \kappa^b \, d_w^3, \tag{2.4}$$

where κ^b is the bilayer bending modulus, which we will meet again in §3–5. The strength of this repulsive interaction is thus inversely proportional to κ^b, and has the same d_w^{-3} dependence as the simplified van der Waals attraction of equation (2.1). The fluctuation force is reduced when the bilayers are charged, are under mechanical or osmotic stress, or are supported on solid substrates, since these factors all tend to suppress the undulations. Typical values of κ^b range from 5×10^{-21} J for sodium dodecyl sulphate monolayers, 3.2×10^{-20} J for fluid bilayers of the monoacylglycerol monoelaidin, to as high as 2×10^{-19} J for fluid phosphatidylcholine bilayers. The first of these values is similar to kT, and so fluctuations are very important in such systems, leading to various isotropic solution phases. For phospholipids, on the other hand, where κ^b is of the order of 20–50 kT, fluctuations play a lesser role in phase stability. Thus, isotropic solution phases tend not to occur for phospholipids, in the absence of co-surfactants or other solutes which increase the layer flexibility. The bending elastic modulus depends strongly on the lipid chainlength and interfacial area, and for lipid mixtures can have a lower value than that for either lipid on its own (Ben-Shaul *et al.* 1987).

In the régime where the hydration force is the dominant transverse repulsive force, there is a coupling between the fluctuations and the hydration force, leading to a fluctuation pressure of the form (Rand & Parsegian 1989)

$$P_{fh} = (\pi kT/32\lambda) \sqrt{(P_0/\kappa^b \lambda)} \, e^{-d_w/2\lambda}. \tag{2.5}$$

At distances $d_w \gg \lambda$, this repulsion will dominate the pure hydration pressure, decaying with distance half as quickly as the latter.

For charged bilayers there is an additional electrostatic repulsion term (Cevc 1990). For low surface potentials, the purely coulombic part has the approximate form

$$P_E = P_{E,0} \, e^{-d_w/\lambda_D}, \tag{2.6}$$

where λ_D is the Debye screening length and the constant term $P_{E,0} = (\sigma^2/2\epsilon\epsilon_0)$, where σ is the surface charge density.

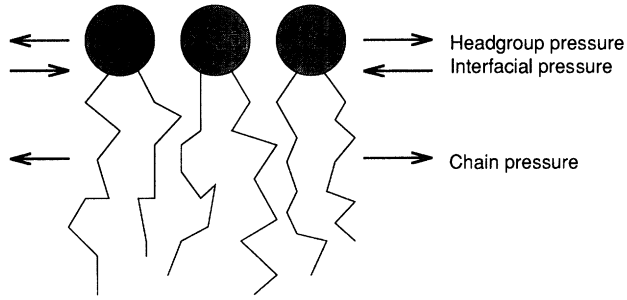

Figure 4. A schematic illustration of the lateral stresses in an amphiphilic monolayer.

For high surface potentials, at reasonably large bilayer separations, the electrostatic repulsive pressure may be approximated by the expression

$$P_{\mathrm{E}} = 6.4 \times 10^4 RTc\,[\tanh\,(zF\Psi_0/2RT)]^2\,\mathrm{e}^{-d_{\mathrm{w}}/\lambda_{\mathrm{D}}}, \tag{2.7}$$

where c is the salt concentration, z is the valency of the charged group, and Ψ_0 is the surface potential of the bilayer, related to the surface charge density via the Gouy–Chapman equation. These expressions neglect hydration, interfacial thickness and charge correlation effects, and are therefore of somewhat restricted validity.

The water layer thickness in the lamellar phase can vary from less than 10 Å to greater than 1000 Å, the swelling to large spacings being driven either by long-range electrostatic or fluctuation forces. In some cases, swelling to very large spacings can also occur in the presence of non-polar solvents such as alkanes, which partition into the bilayers, causing the two lipid monolayers to move apart. Note that in principle, swelling of a lamellar phase with either water or oil could occur at constant interfacial area per molecule.

The rate of lateral diffusion of a phospholipid molecule within the L_α phase is typically 5×10^{-12} m^2 s^{-1}. In addition, rapid chain and headgroup rotation, and conformational changes occur, on timescales of 1–5 ns and 10–100 ps respectively. Diffusion of the lipid molecules across the bilayer ('flip-flop') is usually a much slower process, occurring on a timescale of minutes or hours.

3. Curvature and frustration

All the phases which remain to be discussed are characterized by having curved interfaces. Therefore to understand how such phases form and how they are stabilized we will need to explain the causes of this desire for interfacial curvature.

The physical forces driving the lamellar to non-lamellar phase transition are present in the L_α phase even when we are not close to the phase boundary. This occurs because of imbalances which develop in the lateral stresses (pressures and tensions) occurring around the headgroup region, the polar/non-polar interface, and the hydrocarbon chain region, figure 4. The repulsive lateral pressure in the chain region is due to the thermally activated *cis–trans* rotations in the C–C bonds, which impart momentum to neighbouring amphiphiles during collisions. The hydrophobic effect results in an interfacial tension, γ, which acts to minimize the hydrocarbon–water contact area. The lateral stress around the headgroup is thought to be net repulsive, the outward pressure being due to steric, hydrational and electrostatic interactions, with possible attractive components arising from direct hydrogen

PHILOSOPHICAL TRANSACTIONS OF THE ROYAL SOCIETY A MATHEMATICAL, PHYSICAL & ENGINEERING SCIENCES

Figure 5

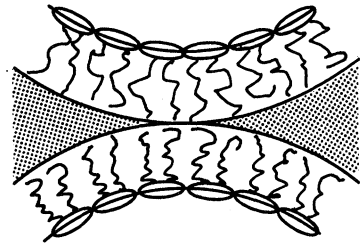

Figure 6

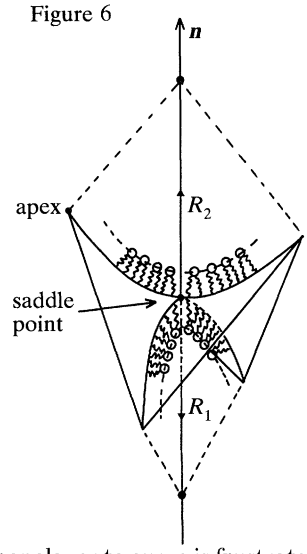

Figure 5. Curvature frustration. The desire for each monolayer to curve is frustrated in the lamellar phase, since it would give rise to voids in the interior of the bilayer. Adapted from Sadoc & Charvolin (1986).

Figure 6. Measurement of surface curvature. A unit vector $\boldsymbol{n}$ is drawn perpendicular to the surface. A plane coincident with $\boldsymbol{n}$ intersects the surface in a curve, whose curvature varies continuously upon rotation of the plane around $\boldsymbol{n}$. The minimum and maximum values of the curvature, noting the sign implied by $\boldsymbol{n}$, are the principal curvatures c_1 and c_2.

bonding between headgroups. The precise details of the headgroup interactions are still poorly understood.

Without, for the moment, worrying too much about the precise form of the lateral interactions, let us consider the effect these stresses will have on a flat monolayer. We can see that because the interactions occur at different depths within the monolayer there will, in general, be a net bending moment acting on the sheet. Where the lateral stress in the headgroup region outweighs that in the chain region, the monolayer will curl towards the chain region. For the opposite case, where the chain pressure is dominant, the curvature will be towards the aqueous region. It is this latter case that we would anticipate leads to the inverse topology phases.

Of course, in the lamellar, bilayer state, this desire for monolayer curvature is physically frustrated. If we consider the case of interfacial curvature towards the water region, it is clear that voids would be exposed in the core of the bilayer, figure 5. This would be energetically prohibitively expensive. There are only a limited number of ways in which the system can relieve this frustration. Using topological arguments Sadoc & Charvolin (1986) have identified four ways in which the system may relax.

1. Where the desire for a curved interface is not too great, the bilayer will remain flat and store the curvature energy by lateral stretching and transverse thinning of the bilayer. The stretching energy per unit area, g_A, is given by

$$g_A = \tfrac{1}{2}\kappa_A(A/A_0 - 1)^2, \tag{3.1}$$

where A is the actual molecular area, A_0 is the optimum area per molecule and κ_A is the isothermal lateral compression modulus (Evans & Skalak 1980). Typically, for a fluid lipid bilayer $\kappa_A \approx 140$ mN m^{-1}. In other words, lipid bilayers are quite stiff to

stretching, reflecting, in part, the large hydrophobic energy cost of increasing the area of exposed hydrocarbon chain, and this in turn means that molecular area changes in the lamellar phase are relatively small and limited. Beyond this stretching limit the material has no choice other than to undergo a phase transition where the stored curvature energy can be relaxed.

2. One choice the system may make, is to form a single continuous bilayer of negative gaussian curvature. This will result in the formation of the porous structures of the inverse bicontinuous cubics.

3. A further choice is to form an infinite number of infinite disconnected aggregates. This corresponds to the cylindrical aggregates of the H_{II} phase.

4. Finally, where the desire for interfacial curvature is at its strongest, the system is likely to create an infinite number of disconnected aggregates of finite size. Apart from the familiar case of inverse micellar solutions, this might also lead to liquid crystalline phases of inverse micelles packed on to specific cubic lattices.

As it stands, our explanation of the forces which drive the lamellar phase towards phases with curved interfaces is purely qualitative. We need to derive an expression which relates the lateral interactions we have described to the local geometry. In other words we require an expression for the curvature free energy, which we can relate back to local molecular interactions. The curvature free energy has been expressed in a number of ways by different authors (see, for example, Helfrich 1973, 1981; Petrov & Bivas 1985; Meunier *et al.* 1987; Dubois-Violette & Pansu 1990; Helfrich & Rennschuh 1990; Fogden *et al.* 1991; Lipowsky 1991; Prost & Rondolez 1991; Ström & Anderson 1992; Ljunggren & Eriksson 1992). However, most of these derive from the original work of Helfrich and we therefore feel it is appropriate to start our discussions using the original expression due to him.

For curvatures which lie within the elastic regime, the curvature free energy per unit area, g_c, of a thin and two-dimensionally isotropic sheet can be expressed as

$$g_c = 2\kappa(H-H_0)^2+\kappa_G K. \tag{3.2}$$

H and K are the mean and gaussian curvatures respectively and are given by

$$H = \tfrac{1}{2}(c_1+c_2), \tag{3.3}$$

$$K = c_1 c_2, \tag{3.4}$$

where c_1 and c_2 are the principal curvatures, figure 6. The coefficient κ is the splay or mean curvature modulus introduced in equation (2.4), κ_G is the saddle splay or gaussian curvature modulus and H_0 is the spontaneous mean curvature, i.e. the mean curvature of the relaxed film. By convention we make the sign of the mean curvature negative if the curvature of the interface is towards the water and vice versa if the curvature is away from the water. This convention will make H at the polar/non-polar interfaces negative for all type II, inverse mesophases. The reader should note that some authors use the convention that positive H represents inverse phases.

It is important to realize that (3.2) can be used to express the curvature elasticity of the bilayer, or the monolayer. However, the meaning of the moduli and the spontaneous curvature will be different. In the case of a symmetric bilayer H_0 must be zero, since both monolayers wish to curve equally in opposite directions, whereas if we consider each monolayer independently H_0 will in general be non-zero. The splay modulus for the bilayer is simply twice that of the monolayer; the cost of cylindrically bending two elastic sheets costs twice that for one. The relation between the bilayer and monolayer saddle splay modulus is however more complex. As

determined by a number of authors (see, for example, Porte *et al.* 1989; Ljunggren & Eriksson 1992) the relation is given by

$$\kappa_{\mathrm{G}}^{b} = 2(\kappa_{\mathrm{G}} - 4\kappa H_0 l), \tag{3.5}$$

where the superscript b indicates a bilayer property, no superscript indicates a monolayer property and l is the monolayer width. We shall return to the meaning of this equation in §5.

The form of the lateral stress profile sets the values of the elastic moduli and the spontaneous curvature via the following integrals taken across either the monolayer or the bilayer ((3.6) and (3.7) are due to Helfrich (1981) and (3.8) is due to Szleifer *et al.* (1990*a*))

$$\kappa H_0 = -\tfrac{1}{2}\int \tau(z)\, z \,\mathrm{d}z, \tag{3.6}$$

$$\kappa_{\mathrm{G}} = \int \tau(z)\, z^2 \,\mathrm{d}z, \tag{3.7}$$

$$\kappa = \frac{1}{2}\int \left(\frac{\partial \tau}{\partial H}\right) z \,\mathrm{d}z. \tag{3.8}$$

Here $\tau(z)$ is the lateral stress at a distance z through the film, figure 7. In principle, these integral equations provide the link between the lateral forces and the interfacial curvature. The ultimate goal of our work is to use experimental determinations of these quantities to work back to a determination of the stress profile. From the form of the stress profile we can then test and develop models of the intermolecular interactions which give rise to the stress profile.

As one might anticipate this ambition is some way off being realized. At present there is still much debate (and indeed confusion) concerning the modelling of the energetics of mesophase behaviour. This has given rise to a proliferation of interpretations, too numerous to cover in this paper. What we have done as a result is to limit our discussions of the hexagonal, bicontinuous cubic and the micellar cubic phases to those models which we have found most useful in understanding and interpreting our own experimental data.

4. The inverse hexagonal phase

The $\mathrm{H_{II}}$ phase is the most common inverse phase possessing interfacial curvature. Using equation(3.2) and measuring the curvature of the $\mathrm{H_{II}}$ monolayer tube at the oil/water interface, the curvature energy can be expressed as

$$g_{\mathrm{c}} = 2\kappa(H^{\mathrm{i}} - H_0^{\mathrm{i}})^2, \tag{4.1}$$

where the superscript i indicates a measurement at the interface, and there is no gaussian curvature term since $c_2^{\mathrm{i}} = 0$. However, the total free energy is not, in general, dominated by the curvature free energy. Inspection of figure 8 shows why. The hexagonal disposition of each $\mathrm{H_{II}}$ water channel means that it is only possible to sustain a relatively narrow range of uniform H^{i} without paying a large vacuum energy cost because of the voids which would form at the corners of the hexagonal cell. Even within the acceptable range of H^{i} the hydrocarbon chains will have to stretch to reach the corners. Both the uniformity of H^{i} and this hydrocarbon stretching have been experimentally confirmed by Turner *et al.* (1992). The physically realizable values of H^{i} inevitably bring the monolayer films on opposite sides of the water channel into close proximity and this will mean that hydration forces, Van der Waals attraction and for charged lipids, electrostatic forces, will also form a significant part of the total free energy.

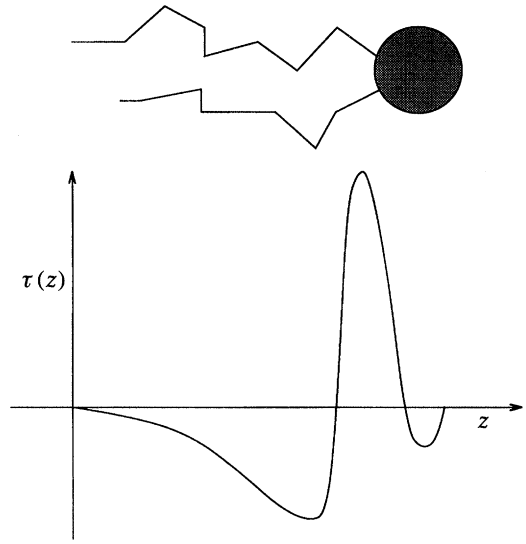

Figure 7. The lateral stress profile $\tau(z)$ across a monolayer.

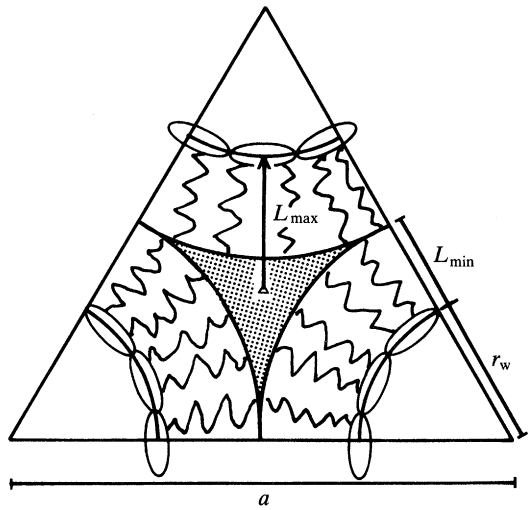

Figure 8. Packing frustration in the H_{II} phase. The shaded region shows the potential void within the hydrocarbon region which must be filled by chains stretching beyond their preferred length. Taken with permission from Seddon (1990).

Kirk *et al.* (1984) have developed a thermodynamic model of the L_α–H_{II} transition in which some of these contributions have been calculated. Their model was used to determine the dependence of these free energy contributions on water concentration.

Equation (4.1) is not likely to remain valid at low hydration, given the constraint that this expression for the curvature free energy is only valid when the film thickness is much smaller than the radius of curvature. Indeed, the osmotic stress measurements of Rand *et al.* (1990) on dioleolyphosphatidylethanolamine (DOPE) and 3/1 DOPE/dioleolyphosphatidylcholine (DOPC) plus alkane have shown that the quadratic dependence of the free energy on H^i only holds when the system is relaxed, i.e. when H^i is close to H^i_0 at full hydration. At reduced hydration where H^i has a larger magnitude, the free energy rises much more steeply than expected, and

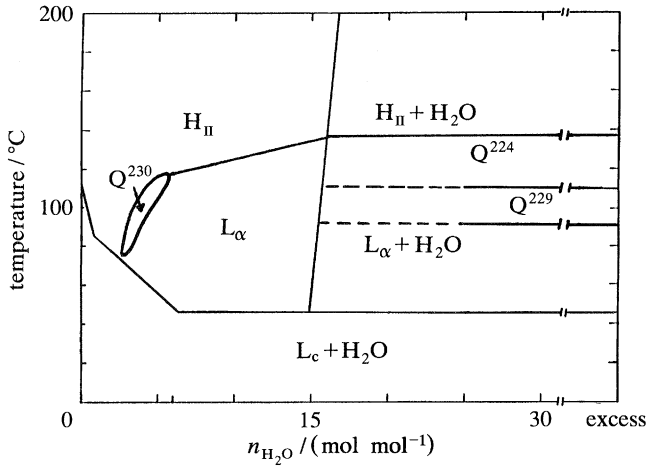

Figure 9. The binary phase diagram for DDPE in water. Taken with permission from Seddon *et al.* (1990*a*).

this is thought to relate to the work of headgroup dehydration, i.e. a breakdown in the first order curvature elastic approximation.

5. The inverse bicontinuous cubic phases

Historically, the inverse bicontinuous cubic phases have often been referred to as intermediate cubic phases. This has served to describe their frequently observed position in the phase diagram, intermediate between the lamellar and inverse hexagonal phase. An example of an actual lipid system which adopts all three of the intermediate bicontinuous cubic phases is the phospholipid didodecyl phosphatidylethanolamine (DDPE), whose binary phase diagram in water (Seddon *et al.* 1984, 1990*a*) is shown in figure 9. It is an important aspect of such phase diagrams, that the intermediate phases are typified by occupying narrow regions of stability.

In these positions on the phase diagram the cubic phases are also intermediate in the sense that their interfacial mean curvature lies between that of the lamellar and inverse hexagonal phase. To prove this assertion and to develop a curvature free energy model of these phases we have to come to grips with their geometry and topology.

It was first suggested by Scriven (1976, 1977) that bicontinuous cubic phases might occur which were based on the periodic minimal surfaces of Schwarz (1865) and those who followed (see, for example, Neovius 1883; Schoen 1970; Nitsche 1989). Such surfaces have the property that $H = 0$ everywhere on the surface. This is achieved by ensuring that $c_1 = -c_2$ at all points, which means that the surface has negative gaussian curvature, $K = -c_1^2$. Such surfaces are hyperbolic, that is, they are saddle surfaces. A saddle surface with quadrilateral edges set by the face diagonals of two side by side cubes can, by appropriate reflections and rotations, be tesselated in space to create Schwarz's P surface, figure 10*a*. The saddle used to create the P surface can also be bent into two new quadrilateral saddles, using the Bonnet transformation, which can then be used to create two further periodic minimal surfaces, the D and G surfaces, figure 10*b*, *c*. This transformation occurs in such a way as to leave the gaussian curvature at all points unchanged, and to preserve all angles, distances and areas on the surface (Andersson *et al.* 1988).

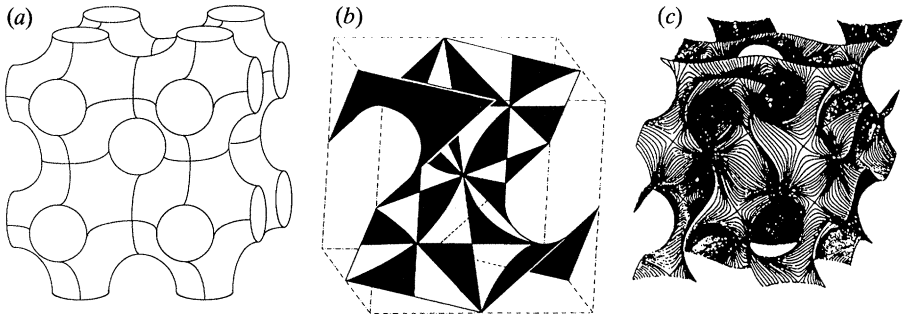

Figure 10. The topologically equivalent family of infinitely periodic minimal surfaces which underlie the bicontinuous cubic phases shown in figure 3. (*a*) Schwarz's P surface. (*b*) Schwarz's D surface (taken with permission from Mackay & Klinowski 1986). (*c*) Schoen's gyroid, and G surface (reproduced from the frontispiece of Dubois-Violette & Pansu 1990).

It is now generally accepted that such periodic minimal surfaces do indeed define the underlying geometry of the bicontinuous cubic phases, with the P surface being the basis for the Im3m cubic phase of figure 3*c*, the D surface relating to the Pn3m cubic phase of figure 3*b* and the G surface defining the geometry of the Ia3d cubic phase of figure 3*a*. Discussion of these ideas and the evidence in support of these structures can be found in numerous articles (see, for example, Longley & McIntosh 1983; Hyde *et al.* 1984; Charvolin 1985; Mackay 1985; Sadoc & Charvolin 1986; Helfrich & Harbich 1987; Andersson *et al.* 1988; Anderson *et al.* 1988; Mariani *et al.* 1988; Hyde 1989; Dubois-Violette & Pansu 1990). In the case of the type II bicontinuous cubics the periodic minimal surface lies along the middle of the bilayer, symmetrically partitioning equal volumes of water and lipid within the unit cell. It can be shown (Hyde 1989) that the area of a small patch, A, on a parallel surface at a distance l on either side of the minimal surface is related to the projected area, A_0, of the patch on the minimal surface by

$$A \approx A_0(1+Kl^2) \tag{5.1}$$

so long as l is not large with respect to the principal curvatures. Since K is always negative (apart from special flat points) we can see that $A \leqslant A_0$. This means that for any inverse bicontinuous cubic phase based on a minimal surface we can accommodate negative H^{i}. The interfacial mean curvature at a distance l from the underlying minimal surface is given by

$$H^{\mathrm{i}} \approx Kl, \tag{5.2}$$

where K is the gaussian curvature on the minimal surface and $c_1 l \ll 1$. The sign on l is determined by placing a vector, with its origin at the polar/apolar interface, such that it points to the ends of the hydrocarbon chains. Any distance measured from the origin in the direction of the vector is then positive and if measured in the reverse direction is negative. This ensures that, in accord with our convention, the correct sign is calculated for H^{i}.

The bicontinuous cubic phases do not suffer the extreme chain packing stress of the $\mathrm{H_{II}}$ phase. Nevertheless their geometry does not fully avoid physical frustration. For the case of the oil/water interface being parallel to the underlying minimal surface we can see from equation (5.2) that H^{i} will vary over the surface. Referring to figure 6, this is because $K = 0$ at the apexes of the fundamental saddle, and varies continuously to a most negative value at the saddle point. This means that $H^{\mathrm{i}} = 0$

near the apexes and is most negative around the saddle points; for a parallel interface the system is curvature frustrated.

We might instead insist that H^{i} be kept constant. To do this the bilayer must be thinned down near the apexes, so that molecules in this region have their chain splay increased, and thickened close to the saddle point, to decrease chain splay where previously it was maximal. (Note that equations (5.1) and (5.2) apply only to parallel surfaces, and therefore are not applicable here.) Now having cured the curvature frustration we have introduced transverse chain stress, by varying the bilayer width. Anderson *et al.* (1988) have calculated that where the magnitude of $1/H^{\mathrm{i}}$ is significantly greater than l, the variation in bilayer width can be very small and the free energy price of variations in the chain length will be less than in the $\mathrm{H_{II}}$ phase.

We therefore anticipate that we may assume a constant thickness bilayer in using the Helfrich expression, equation (3.2), for the curvature free energy of the cubic phase. In using the Helfrich expression we effectively collapse the bilayer on to the minimal surface, the effects of the bilayer thickness being subsumed into the curvature elastic parameters. If we consider the expression in terms of the bilayer and make the origin of all our calculations the underlying minimal surface we see that both H^b and H_0^b are, by definition zero. This means that the curvature free energy is simply proportional to K. The saddle splay modulus must be positive if we are to obtain bicontinuous structures since here $K \leqslant 0$. This means that we can reduce the free energy simply by making K more negative. Geometrically this is equivalent to reducing the dimensions of the cubic unit cell. This would presumably proceed until compensating interbilayer repulsive forces stabilized the phase.

In a cubic phase of uncharged lipids, the only significant repulsive bilayer interaction across the aqueous channels is that due to the hydration force, which would give rise to water channels with diameters at the narrowest parts of the phase of a few tens of ångstroms. (Non-lamellar phases are always geometrically stiffened and in the bicontinuous cubics the bilayer fluctuations appear as acoustic and optical lattice modes (Bruinsma 1992).) However, experimentally we can observe swollen bicontinuous cubic phases with water channels which are, at their narrowest, over 100 Å in diameter (Ström & Anderson 1992; Templer *et al.* 1992*a*). In such phases all bilayer–bilayer interaction terms such as the attractive van der Waals and the repulsive hydration force must be negligible (see equation (2.3)). Therefore, it is clear that we are missing a stabilizing term in the curvature free energy expression.

Many extensions have been made to Helfrich's original equation; for example Fogden *et al.* (1991) have shown how a spontaneous gaussian curvature may be introduced to produce a stable solution to the equation. However, we do not feel it would serve any useful purpose to discuss every stabilized curvature free energy model here, indeed we suspect it might serve to confuse rather than elucidate. Rather, we present our own idiosyncratic synthesis of the work of Ljunggren & Eriksson (1992) which itself follows Helfrich's original work and has close similarities to the work of Helfrich & Rennschuh (1990). In Ljunggren & Eriksson's model the curvature free energy is expanded up to fourth order in the principal curvatures, making the bilayer curvature free energy for a bicontinuous cubic phase

$$g_{\mathrm{c}}^b = \kappa_{\mathrm{G}}^b K + \kappa_{\mathrm{G}}^{b'} K^2, \tag{5.3}$$

where the second-order saddle splay modulus, $\kappa_{\mathrm{G}}^{b'}$ can be related to monolayer quantities by (J. C. Eriksson, personal communication)

$$\kappa_{\mathrm{G}}^{b'} = 4\kappa l^2, \tag{5.4}$$

where all symbols are as before.

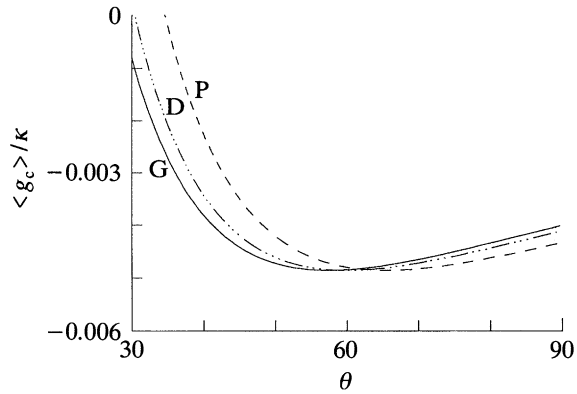

Figure 11. The curvature elastic free energy per unit area as a function of hydration. The curvature free energy divided by the splay modulus, calculated for the G, D and P surfaces, has been evaluated using $H_0 = -8.3 \times 10^{-3}$ Å^{-1}, $\kappa_G/\kappa = 0.015$, $A = 116$ Å^2, $l = 15.4$ Å and $v = 1771$ Å^3.

Since both of the saddle splay moduli are positive, equation (5.3) clearly satisfies the condition that we should have a stable minimum in the free energy with respect to K. Remembering that K varies continuously over the minimal surface we evaluate the surface averaged bilayer curvature free energy per unit area as

$$\langle g_c^b \rangle = \kappa_G^b \frac{2\pi\chi}{S_u} + \kappa_G^{b'} \frac{4\pi^2\chi^2 \langle K^2 \rangle}{S_u^2 \langle K \rangle^2}. \tag{5.5}$$

S_u is the surface area of the underlying minimal surface, χ is the Euler characteristic of the unit cell and has values of -2, -4 and -8 for the D, P and G surfaces respectively, and $\langle \ldots \rangle$ indicates a surface averaged quantity. Since all of the surfaces are related by a Bonnet transformation, $\langle K^2 \rangle / \langle K \rangle^2$ is a constant, which has been evaluated by Helfrich & Rennschuh (1990) to be 1.2187 (henceforth denoted f). Using topological and geometrical relations (Hyde 1989) it is possible to show that the surface averaged curvature free energy expressed in terms of monolayer quantities is given by

$$\langle g_c^b \rangle = \frac{6}{l^2}\left(\frac{1-I}{3I-1}\right)\left[\kappa_G - 4\kappa H_0 l + 6\kappa f\left(\frac{1-I}{3I-1}\right)\right], \tag{5.6}$$

where $I = v/Al$, the molecular volume divided by the headgroup area and the monolayer width. As was pointed out previously the local geometry and topology of the D, P and G surfaces is the same, which means that we should anticipate that the energetic minima for the curvature free energy in these phases will always be degenerate. However, they are distinguished by packing space differently, that is, the dimensionless surface area $\sigma = S_u/V_u^{\frac{2}{3}}$ varies ($\sigma_G = 3.091$, $\sigma_P = 2.345$ and $\sigma_D = 1.919$). Using these relationships we can determine the local molecular geometry, I, in a given phase with respect to the ratio of moles of water to moles of lipid, θ.

$$\theta = \frac{v}{29.9}\left[\sqrt{\left[\frac{\pi\chi(3I-1)^3}{24\sigma^3 I^2(1-I)}\right]} - 1\right], \tag{5.7}$$

where the value of 29.9 is the volume of a water molecule in cubic ångströms.

The curvature free energy as a function of hydration can be determined from equations (5.6) and (5.7). The graph in figure 11 arose from a preliminary

determination of elastic parameters in a ternary system of dilauroylphosphatidylcholine and lauric acid, at a molar ratio of 1:2, in water. A more complete description of this work is in preparation. The graph is typical of the phase sequence commonly observed for the bicontinuous cubics. The Ia3d cubic, based on the G surface, appears at the lowest hydration since it packs space most efficiently. The Pn3m cubic appears next, although only fleetingly in this example (experimentally we were unable to resolve this phase), followed by the Im3m cubic, based on the P surface, which has the most open structure. At low hydration the curvature free energy rises steeply, so we might well expect that the H_{II} phase will have a lower free energy than Ia3d at low hydrations (in reality this occurs around $\theta = 30$ for this system). The curvature free energy difference between the phases is small, which is typical of such phase transitions.

A note of caution should be sounded here. The fundamental aim behind fitting the experimentally determined free energy functional to theory is to determine the lateral stress profile via equations (3.6), (3.7) and (3.8). This means that one must ensure that the measured free energy is predominantly due to the curvature component. This will hold true only where the lattice parameter is sufficiently large compared with l. One can of course approximate any free energy curve close to the minimum by equations such as (5.6), but the elastic parameters derived in this way inevitably include contributions from transverse interactions such as the hydration force and van der Waals interactions. No transverse interaction terms have yet been calculated for these complex geometrical surfaces.

A second point that should be made is that equation (5.6) is a function of v/Al (I), and of l. This might be problematic in making any calculation, since although I is fixed at any level of hydration, l can be varied within obvious, physical limits, as long as v and A change in such a way as to keep I constant. Fortunately v is, to first order, constant in real systems, and there exists a surface, approximately parallel to the underlying minimal surface (Anderson *et al.* 1988) about which the average molecular area does not vary. This is the neutral surface and it lies in the chain region close to the position of maximum chain pressure, usually somewhere between the oil/water interface and the third carbon atom along the aliphatic chain (see, for example, Szleifer *et al.* 1990*b*). By introducing this invariant area, A_n, it becomes possible to express I in terms of only one variable, l.

Thus far in this section, we have shown how the curvature free energy expression behaves as a function of the hydration in a bicontinuous cubic phase. We are not yet able to predict the behaviour as a function of temperature (the ordinate in figure 9). To date only the lateral stress in the chain region has been theoretically treated at a molecular level (Szleifer *et al.* 1990*a*, *b*). However, since the coordinate origin of all of our calculations lies on the minimal surface, the contribution from the interfacial and headgroup lateral stresses is heavily weighted in the higher moments of the stress profile (equations (3.6)–(3.8)). It might be argued that simply by moving the origin of the integration of the lateral stress to the interface we could reduce the contribution of these difficult to model stresses to negligible levels. Unfortunately we cannot avoid the problem so easily, since we can only have one origin for our integration and the interface and headgroup on the other side of the bilayer would now be even further away from the origin.

This problem can be seen in the expression for the first order bilayer saddle splay modulus (equation (3.5)); κ_G^b is not simply twice the monolayer gaussian modulus. If it was we could quite happily calculate κ_G from any position along the monolayer

PHILOSOPHICAL TRANSACTIONS OF THE ROYAL SOCIETY A MATHEMATICAL, PHYSICAL & ENGINEERING SCIENCES

stress profile, but there is an additional contribution which expresses the fact that the bilayer might wish to adopt negative gaussian curvature even if the individual monolayers do not. The bilayer saddle splay modulus can then be seen to be composed of two distinct parts. The term $-4\kappa H_0 l$ expresses how the desire for monolayer, mean interfacial curvature alone can be satisfied by deforming the bilayer on to a saddle, whilst the second, more intriguing term, counts the cost (or otherwise) of deforming the monolayer on to a saddle. Since H_0 is negative, the mean curvature term is always positive. Hence, we can still have a positive value of κ_G^b even if it is energetically unfavourable to deform the monolayer towards a saddle surface, i.e. negative κ_G. In this case the bicontinuous phases are being driven entirely by a desire for mean interfacial curvature. We would expect that this might lead to rather narrow ranges of phase stability since the magnitude H_0 would have to be great enough to make κ_G^b positive, and where the magnitude of H_0 is great we should expect to find an H_{II} phase close by. Thus for this situation we should expect to find narrow regions of stability and relatively small cubic lattice parameters. This is indeed the case in the systems which have the appearance of that shown in figure 9.

For DDPE the cubic phases are suppressed in favour of the H_{II} phase upon addition of small amounts of dodecane. This presumably occurs because DDPE has a strong desire for mean interfacial curvature and relatively little desire for gaussian curvature, i.e. κ_G is small or possibly negative. Hence by reducing the potential packing strain in the H_{II} phase by adding alkane the H_{II} phase is favoured. All three cubic phases lie between the L_α and H_{II} phases, with Ia3d appearing at low water content, and Im3m and Pn3m occurring on heating in excess water (the limiting hydrations of the latter two phases are not precisely established, but are in the region of 50% (by mass) water). A striking result is that although the latter two cubic phases are inverse, they are actually more hydrated than the L_α phase. We presume that this is because the lattice parameter is set by the interfacial mean curvature, as is implicit in equations (5.6) and (5.7). Hence for intermediate values of H^i extra water is needed to fill the aqueous volume created in the new topology. What we cannot explain is why there is apparently a region in the phase diagram, between 5 and 15 moles of water per moles of lipid, where the cubic phases disappear as an intermediate phase.

What if κ_G is positive? Clearly in this case we should expect to see a greater range of cubic phase stability and the possibility of larger lattice parameters. From a consideration of the lateral stress profile, we would expect positive values of κ_G if the headgroup stress was rather small, or even attractive. The monoglycerides, which have small headgroups and have been shown to exhibit headgroup–headgroup hydrogen bonding (Nilsson *et al.* 1991), are indeed characterized by having large parts of their phase diagrams occupied by cubic phases, as shown in figure 12.

In this case the addition of dodecane, up to the maximum measured dodecane mole fraction of 0.16, does not apparently lead to the destabilization of the cubic phases (Moriarty 1992). We presume that this is because κ_G is positive and relatively large. Support for these ideas comes from the observation that the addition of a second lipid component which only forms lamellar phases, DOPC, can act to preferentially reduce the magnitude of H_0 and so form swollen cubic phases (Templer *et al.* 1992*a*) up to size limits sets by κ (Bruinsma 1992).

As suggested by Bouligand (1990) saddle surfaces could be induced to form in membranes by components which disrupt the regular lipid packing of a bilayer. This could occur for example in a roughly hexagonal packing of lipids, in the presence of

PHILOSOPHICAL TRANSACTIONS OF THE ROYAL SOCIETY A MATHEMATICAL, PHYSICAL & ENGINEERING SCIENCES

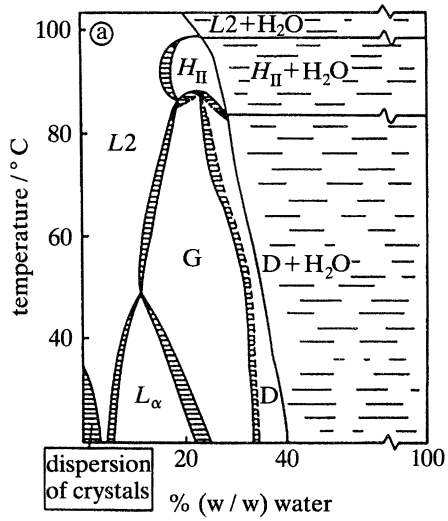

Figure 12. The binary phase diagram of mono-olein in water. Taken with permission from Hyde *et al.* (1984).

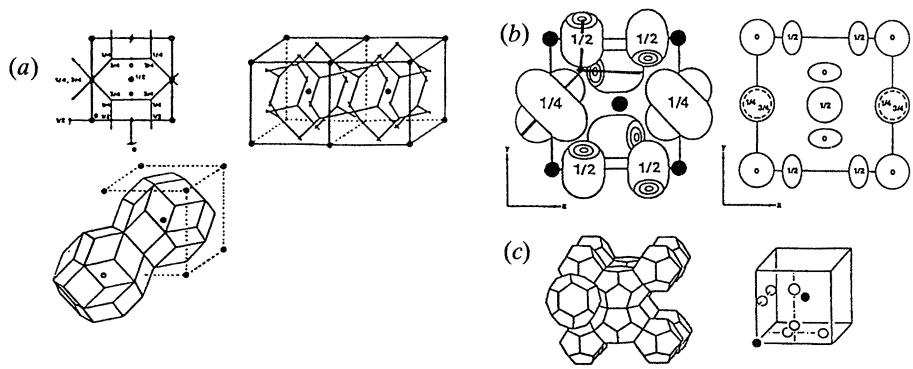

Figure 13. Three proposed structures for the Pm3n micellar cubic phase. (*a*) The rod/micelle model of Tardieu & Luzzati (1970), which has now been discarded. (*b*) The rod-like model of Fontell *et al.* (1985). (*c*) The 'clathrate-like' model of Charvolin & Sadoc (1988). Taken with permission from Fontell (1990).

a low density of somewhat larger proteins having seven-fold coordination to the neighbouring lipids, which would induce a saddle deformation of the bilayer. Such coordination at saddle points is also used to create the proposed bicontinuous versions of fullerenes (Terrones & Mackay 1992). Such ideas suggest that amphiphiles having effective headgroup shapes which can pack tightly around the disclination at a saddle point as well as the flat, umbilic points might promote the stability of the bicontinuous phases by lowering the hydrophobic energy cost.

6. The discontinuous (micellar and inverse micellar) cubic phases

In addition to the bicontinuous cubic phases, with negative gaussian interfacial curvature, there is another class of cubic phases having *positive* gaussian interfacial curvature. For these cubic phases the magnitudes of the average mean interfacial curvatures (positive or negative) exceed those not only of the bicontinuous cubic phases, but also those of the hexagonal H_I and H_{II} phases.

PHILOSOPHICAL TRANSACTIONS OF THE ROYAL SOCIETY A MATHEMATICAL, PHYSICAL & ENGINEERING SCIENCES

Many binary surfactant/water systems adopt one or more type I cubic phases adjacent to the micellar solution at volume fractions roughly in the region of 0.5. Such behaviour is not generally seen with phospholipids, apart from the single chain lysoderivatives (Arvidson *et al.* 1985). The most common of these cubic phases is of spacegroup Pm3n (no. 223), and its structure has been the subject of considerable controversy. The initial suggestion (Tardieu & Luzzati 1970) consisted of a combination of micelles and a connected network of lipid rods, as shown in figure 13*a*. However, the structure is now accepted to consist of a packing of two types of discrete micellar aggregates, two of one type and six of the other per unit cell (Vargas *et al.* 1992). It is not yet established whether the aggregates are short rods with differing rotational freedom at the two non-equivalent sites (Fontell *et al.* 1985), as shown in figure 13*b*, or whether one site has quasi-spherical aggregates, and the other discoidal aggregates (Charvolin & Sadoc, 1988), as shown in figure 13*c*.

Certain surfactant systems, such as the polyoxyethylene surfactants, can adopt as many as three distinct cubic phase structures in the region of the phase diagram adjacent to the micellar solution (R. J. Mirkin, J. M. Seddon & G. J. T. Tiddy, unpublished results). Presumably all of these structures are based on packings of discrete micellar aggregates, although the detailed structures are not yet established.

Cubic structures based on packings of inverse micelles have often been suggested in the past, but have usually turned out to be *bicontinuous* cubic phases, and a feeling developed in recent years that the former structures might actually be inherently unstable. However, the first example of such an inverse micellar cubic phase, of space group Fd3m (no. 227) has now been established in various hydrated binary lipid mixtures (Mariani *et al.* 1988, 1990; Seddon 1990*b*; Seddon *et al.* 1990*b*). The amphiphile systems range from fatty-acid–soap, fatty-acid–monoglyceride, to diglyceride–phospholipid mixtures. The common feature of these systems is that they contain one relatively strongly hydrophilic species, but large amounts of another species that is too weakly hydrophilic to form any lyotropic mesophases at all on its own in water. The latter species must however have the capacity for hydrogen-bonding in its headgroup, presumably to enhance its miscibility with the more polar lipid, and to ensure that it locates with its headgroup at the polar/non-polar interface. No example has as yet been found of a purely binary lipid/water system forming the Fd3m inverse micellar cubic phase. It is important to note that, unlike the micellar cubic phase Pm3n, the Fd3m cubic phase is frequently stable in the presence of an excess water phase.

The structure of this Fd3m cubic phase has recently been solved by low-resolution crystallography (Luzzati *et al.* 1992), and consists of a complex packing of two types of quasi-spherical inverse micelles, as shown in figure 14 (the previously proposed structure (Mariani *et al.* 1988, 1990) is now known to be incorrect). There are eight of the larger, and 16 of the smaller inverse micelles per unit cell. It is remarkable that essentially this structure was previously predicted, based on a theoretical consideration of the properties of intersecting fluid films (Charvolin & Sadoc 1988).

The role of the weakly polar component appears to be twofold. First, it strongly increases the tendency of the interface to curve towards the water. This is partly due to its low hydrophilicity, but may also be due to a partial dehydration of the headgroup of the more polar species from headgroup–headgroup bonding. Secondly, it provides a mechanism for the stabilization of two different sizes of inverse micelle, which would be energetically unfavourable for a binary lipid/water system, by preferentially partitioning into the smaller, more highly curved inverse micelles.

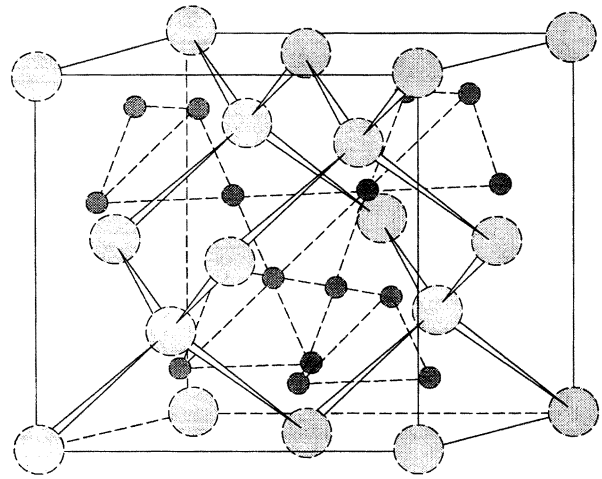

Figure 14. The Fd3m inverse micellar cubic phase structure. The light and dark shaded spheres represent the larger and smaller water cores of the inverse micelles. The remaining volume is filled with fluid hydrocarbon chains. The connecting lines are drawn merely to guide the eye. Taken with permission from Seddon *et al.* (1990*b*).

The effect of lowering the lipid chainlength is to suppress the formation of the Fd3m cubic phase, replacing it with an H_{II} phase (Seddon & Bartle 1992). This is precisely the opposite behaviour to that of the inverse bicontinuous cubic phases, which are favoured by lowering the chainlength (Seddon *et al.* 1984, 1990*a*). However, it is entirely consistent with the inverse micellar structure of Fd3m, which has a more negative interfacial mean curvature, but more chain packing frustration, than the H_{II} phase. This increased packing frustration is partly due to the difference in size of the two types of inverse micelle, and partly to the lower packing fraction of the Fd3m structure (0.71 for an AB_2 packing of hard spheres, with the ratio of the radii of A and B equal to 1.225) compared to that of the hexagonal phase (0.907 for a packing of hard cylinders).

It is interesting to note that the structures of the micellar cubic phase Pm3n (no. 223) and the inverse micellar cubic phase Fd3m (no. 227) are analogous (Charvolin & Sadoc 1988) to those of the so-called 12 Å and 17 Å cubic crystalline clathrate crystals respectively. In the 12 Å clathrate crystal structure, the water forms two dodecahedral and six tetrakaidecahedral cages per unit cell, whereas in the 17 Å structure there are 16 dodecahedral and 8 hexakaidecahedral cages per unit cell. In the Pm3n cubic phase, the two polyhedral surfaces define the mid-region of the water, whereas in the Fd3m cubic phase the corresponding polyhedral surfaces define the mid-region (methyl ends) of the hydrocarbon chains. To date, Pm3n has only been found as a type I phase, and Fd3m only as a type II version. It is not yet clear whether this is purely accidental, or whether there is some underlying reason for this apparent asymmetry.

7. Geometry of non-lamellar phase transitions

In analysing phase transitions between non-lamellar phases, one extremely important, yet little explored aspect is the geometric or epitaxial relations which exist between coexisting lyotropic phases. For lamellar-hexagonal transitions, this epitaxy is nearly self-evident, with the (001) crystallographic planes of the lamellar

PHILOSOPHICAL TRANSACTIONS OF THE ROYAL SOCIETY A MATHEMATICAL, PHYSICAL & ENGINEERING SCIENCES

phase (i.e. the plane of the bilayers) being aligned with the (10) planes of the hexagonal phase (Gruner *et al.* 1985; Templer *et al.* 1992*b*). For transitions involving three-dimensional phases, however, the situation is much more complicated, although it is now becoming clear that well-defined epitaxies also occur. The best studied system to date is the polyoxyethylene surfactant hexaethylene glycol mono-*n*-dodecyl ether ($C_{12}EO_6$). Monodomain samples of this type I system have been studied by X-ray diffraction and polarizing microscopy (Rançon & Charvolin 1988*a*; Clerc *et al.* 1991), and the epitaxy shown in figure 15 was established. The (001) planes of the lamellar phase were aligned parallel to the (211) planes of the Ia3d bicontinuous cubic phase. The H_I phase grew from the cubic phase with its (10) planes parallel to the (211) planes of the latter, and with the H_I cylinder axes aligned along the ⟨111⟩ axes (body-diagonal) of the cubic phase. Furthermore, the repeat spacings of these crystallographic planes (which are the planes of highest density in each phase) were equal for each of the three phases. Similar, precise epitaxies have been observed at the phase boundaries of another type I system, sodium dodecyl sulphate/water (Kékicheff & Cabane 1988). These important findings imply that lyotropic phase transitions occur along well defined geometric paths, and such studies should be most useful in analysing the underlying mechanisms of these transitions.

For type II systems much less information is currently available on cubic phase epitaxies. We have observed in the system monoolein/water (Templer *et al.* 1992*b*) that the alignment of the Ia3d cubic phase with respect to the lamellar phase was with the ⟨111⟩ axis parallel to the lamellae. However, the cubic orientation varied between having the (220) planes or the (211) planes parallel to the lamellae. The latter orientation corresponds to that observed in the type I mesophases. Similar, although not identical results have also been observed by Rawiso & Charvolin (unpublished observations).

Further insight into the mechanism of lyotropic phase transformations may be obtained by analysis of diffuse scattering indicative of defects or displacement disorder, from monodomain samples close to phase transitions (Rançon & Charvolin 1987, 1988*b*).

It has been suggested that cubic–cubic transitions between phases of the same genus, such as Pn3m and Ia3d, might occur via a Bonnet-like transformation (Hyde *et al.* 1984). Such a mechanism is attractive because it leaves the gaussian curvature of the bilayer mid-plane unchanged during the transition, and the underlying minimal surfaces (the D-surface and the G-surface) of the above-mentioned cubic phases are indeed related by the Bonnet transformation. However, it would require a rather complex sequence of layer self-intersections to occur during the transition, and thus is probably physically unrealistic. We believe that a more physical model is that considered for minimal surfaces by Sadoc & Charvolin (1989), where the transformation P–D–G may be achieved simply by changing the connectivity of the nodes of the networks (skeletal graphs) which lie on either side of the minimal surfaces. These three networks are shown in figure 16. The six-fold connectivity of the node for the P-surface can be changed first to the four-fold one of the D-surface, and then to the three-fold one of the G-surface simply by carrying out a stretching process. Concomitant adjustment of the angles between the network lines from 90° to 109.47° to 120° will then achieve the transformation P–F–G. During this process stretching and deformation of the minimal surfaces occurs, but self-intersection of the surfaces is not required. Cubic–cubic transitions occurring by such a mechanism

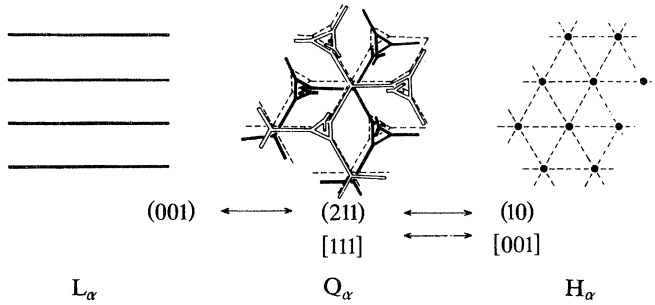

Figure 15. The epitaxial relationships between the L_α, oil-in-water bicontinuous cubic (Ia3d), and H_I phases, observed in the surfactant system $C_{12}EO_6$/water. Taken with permission from Rançon & Charvolin (1988*a*).

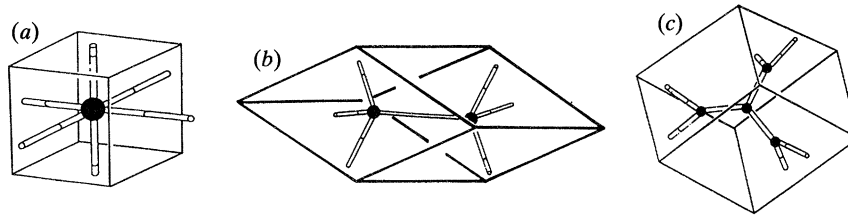

Figure 16. Stretching transformations between the periodic minimal surface family G–D–P. (*a*) The skeletal graph of the P surface unit cell. (*b*) By stretching the six-fold junction along the body diagonal one obtains the two four-fold junctions shown, and with appropriate adjustments of angles, this gives the correct symmetry for the D surface. (*c*) Stretching at each of the four-fold junctions one obtains the three-fold junctions of the gyroid. Taken with permission from Sadoc & Charvolin (1989).

could thus proceed without the need for complex layer fusion events to occur, and such topological stretching may be able to occur in a fluid bilayer with little or no stretching energy.

This work has been supported by grants from the SERC (grant nos GR/F44052, GR/H10672 and GR/H69229), the British Council and the Royal Society, who also supported R.H.T. in the form of a University Research Fellowship. We thank Jan Christer Eriksson, for his help in explaining the mysteries of curvature energy and Jean Charvolin, Alan Mackay, Jean-François Sadoc and Humberto Terrones for their help in understanding the geometry of minimal surface cubic phases. Finally, we acknowledge the efforts of our past and current research students in obtaining the experimental data against which to test our ideas.

References

Anderson, D. M., Gruner, S. M. & Leibler, S. 1988 Geometrical aspects of the frustration in the cubic phases of lyotropic liquid crystals. *Proc. Natn. Acad. Sci. U.S.A.* **85**, 5364–5368.

Andersson, S., Hyde, S. T., Larsson, K. & Lidin, S. 1988 Minimal surfaces and structures: from inorganic and metal crystals to cell membranes and biopolymers. *Chem. Rev.* **88**, 221–242.

Arvidson, G., Brentel, I., Khan, A., Lindblom, G. & Fontell, K. 1985 Phase equilibria in four lysophosphatidylcholine/water systems. Exceptional behaviour of 1-palmitoyl glycerophosphocholine. *Eur. J. Biochem.* **152**, 753–759.

Ben-Shaul, A., Szleifer, L. & Gelbart, W. M. 1987 Molecular theory for amphiphile packing and elastic properties of monolayers and bilayers. In *Physics of amphiphilic layers* (ed. J. Meunier, D. Langevin & N. Boccara), pp. 2–8. Berlin: Springer Verlag.

Bouligand, Y. 1990 Comparative geometry of cytomembranes and water-lipid systems *J. Phys., Paris* **51** (C7), 35–52.

Bruinsma, R. 1992 Elasticity and excitations of minimal crystals. *J. Phys., Paris* II **2**, 425–451.

Cevc, G. 1990 Membrane electrostatics. *Biochim. Biophys. Acta* **1031**, 311–382.

Cevc, G. & Marsh, D. 1987 *Phospholipid bilayers: physical principles and models*. New York: Wiley.

Charvolin, J. 1985 Crystals of interfaces: the cubic phases of amphiphile/water systems. *J. Phys., Paris* **46** (C3), 173–190.

Charvolin, J. & Sadoc, J. F. 1988 Periodic systems of frustrated fluid films and micellar cubic structures in liquid crystals. *J. Phys., Paris* **49**, 521–526.

Charvolin, J. & Tardieu, A. 1978 Lyotropic liquid crystals: structure and molecular motions. *Solid State Phys. Suppl.* **14**, 209–257.

Clerc, M., Levelut, A. M. & Sadoc, J. F. 1991 Transitions between mesophases involving cubic phases in the surfactant-water systems. Epitaxial relations and their consequences in a geometrical framework. *J. Phys., Paris* II **1**, 1263–1276.

Dubois-Violette, E. & Pansu, B. (eds) 1990 International workshop on geometry and interfaces. *J. Phys., Paris* **51** (C7).

Evans, E. & Skalak, R. 1980 *Mechanics and thermodynamics of biomembranes*. Boca Raton, Florida: CRC Press.

Fogden, A., Hyde, S. T. & Lündberg, G. 1991 Bending energy of surfactant films. *J. chem. Soc. Faraday Trans.* **87**, 949–955.

Fontell, K. 1990 Cubic phases in surfactant and surfactant-like lipid systems. *Colloid Polym. Sci.* **268**, 264–285.

Fontell, K., Fox, K. K. & Hansson, E. 1985 On the structure of the cubic phase I_1 in some lipid-water systems. *Molec. Cryst. Liq. Cryst. Lett.* **1**, 9–17.

Gruner, S. M. 1989 Stability of lyotropic phases with curved interfaces. *J. phys. Chem.* **93**, 7562–7570.

Gruner, S. M., Rothschild, K. J. & Clark, N. A. 1982 X-ray diffraction and electron microscope study of phase separation in rod outer segment photoreceptor membrane multilayers. *Biophys. J.* **39**, 241–251.

Helfrich, W. 1973 Elastic properties of lipid bilayers: theory and possible experiments. *Z. Naturforsch.* **28c**, 693–703.

Helfrich, W. 1978 Steric interaction of fluid membranes in multilayer systems. *Z. Naturforsch.* **33a**, 305–315.

Helfrich, W. 1981 Amphiphilic mesophases made of defects. In *Physics of defects* (ed. R. Balian, M. Kléman & J. P. Poirier), pp. 715–755. Amsterdam: North-Holland.

Helfrich, W. & Harbich, W. 1987 Equilibrium configurations of fluid membranes. In *Physics of amphiphilic layers* (ed. J. Meunier, D. Langevin & N. Boccara), pp. 58–63. Berlin: Springer Verlag.

Helfrich, W. & Rennschuh, H. 1990 Landau theory of the lamellar-to-cubic phase transition. *J. Phys., Paris* **51** (C7), 189–195.

Hyde, S. T. 1989 Microstructure of bicontinuous surfactant aggregates. *J. phys. Chem.* **93**, 1458–1464.

Hyde, S. T., Andersson, S., Ericsson, B. & Larsson, K. 1984 A cubic structure consisting of a lipid bilayer forming an infinite periodic minimum surface of the gyroid type in the glycerolmonooleat-water system. *Z. Krystallogr.* **168**, 213–219.

Israelachvili, J. N. 1991 *Intermolecular and surface forces*, 2nd edn. San Diego: Academic Press.

Israelachvili, J. N. & Wennerström, H. Å. 1992 Entropic forces between amphiphilic surfaces in liquids. *J. phys. Chem.* **96**, 520–531.

Kékicheff, P. & Cabane, B. 1988 Crystallography of systems with long periods: a neutron-scattering study of sodium dodecyl sulfate/water mesophases. *Acta crystallogr.* B **44**, 395–406.

Kirk, G. L., Gruner, S. M. & Stein, D. L. 1984 A thermodynamic model of the lamellar to inverse hexagonal phase transition of lipid membrane-water systems. *Biochemistry* **23**, 1093–1102.

Larsson, K. 1989 Cubic lipid-water phases: structures and biomembrane aspects. *J. phys. Chem.* **93**, 7304–7314.

Lindblom, G. & Rilfors, L. 1989 Cubic phases and isotropic structures formed by membrane lipids – possible biological relevance. *Biochim. Biophys. Acta* **988**, 221–256.

PHILOSOPHICAL TRANSACTIONS OF THE ROYAL SOCIETY A MATHEMATICAL, PHYSICAL & ENGINEERING SCIENCES

Lipowsky, R. 1991 The conformation of membranes. *Nature, Lond.* **349**, 475–481.

Ljunggren, S. & Eriksson, J. C. 1992 Minimal surfaces and Winsor II microemulsions. *Langmuir* **8**, 1300–1306.

Longley, W. & McIntosh, T. J. 1983 A bicontinuous tetrahedral structure in a liquid-crystalline lipid. *Nature, Lond.* **303**, 612–614.

Luzzati, V. 1968 X-ray diffraction studies of lipid-water systems. In *Biological membranes*, vol. 1 (ed. D. Chapman), pp. 71–123. London: Academic Press.

Luzzati, V., Vargas, R., Gulik, A., Mariani, P., Seddon, J. M. & Rivas, E. 1992 Lipid polymorphism: a correction. The structure of the cubic phase of extinction Fd-- consists of two disjointed reverse micelles embedded in a three-dimensional hydrocarbon matrix. *Biochemistry* **31**, 279–285.

Mackay, A. L. 1985 Periodic minimal surfaces. *Nature, Lond.* **314**, 604–606.

Mackay, A. L. & Klinowski, J. 1986 Towards a grammar of inorganic structure. *Comp. Math. Appl* **12** B, 803–824.

Mariani, P., Luzzati, V. & Delacroix, H. 1988 Cubic phases of lipid-containing systems. Structure analysis and biological implications. *J. molec. Biol.* **204**, 165–189.

Meunier, J., Langevin, D. & Boccara, N. (eds) 1987 *Physics of amphiphilic layers*. Berlin: Springer-Verlag.

Moriarty, S. 1992 The effect of the addition of oil on the phase behaviour of 1-monooleoyl-rac-glycerol. M.Sc. thesis, Imperial College, London, U.K.

Neovius, E. 1883 *Bestimmung zweier speziellen periodischen minimalflachen*. Helsingfors: J. C. Frenckell and Sons.

Nilsson, A., Holmgren, A. & Lindblom, G. 1991 Fourier-transform infrared spectroscopy study of dioleoylphosphatidylcholine and monooleoylglycerol in lamellar and cubic liquid crystals. *Biochemistry* **30**, 2126–2133.

Nitsche, J. C. C. 1989 *Lectures on minimal surfaces*, vol. 1. Cambridge University Press.

Pascher, I., Lundmark, M., Nyholm, P.-G. & Sundell, S. 1992 Crystal structures of membrane lipids. *Biochim. Biophys. Acta.* **1113**, 339–373.

Petrov, A. G. & Bivas, I. 1985 Elastic and flexoelectric aspects of out-of plane fluctuations in biological and model membranes. *Prog. Surf. Sci.* **16**, 389–511.

Porte, G., Appell, J., Bassereau, P. & Marignan, J. 1989 L_α to L_3: a topology driven transition in phases of infinite fluid membranes. *J. Phys., Paris* **50**, 1335–1347.

Prost, J. & Rondolez, F. 1991 Structures in colloidal physical chemistry. *Nature, Lond.* (Suppl.) **350**, 11–23.

Rançon, Y. & Charvolin, J. 1987 Displacement disorder in a liquid crystalline phase with cubic symmetry. *J. Phys., Paris* **48**, 1067–1073.

Rançon, Y. & Charvolin, J. 1988*a* Epitaxial relationships during phase transformations in a lyotropic liquid crystal. *J. phys. Chem.* **92**, 2646–2651.

Rançon, Y. & Charvolin, J. 1988*b* Fluctuations and phase transformations in a lyotropic liquid crystal. *J. phys. Chem.* **92**, 6339–6344.

Rand, R. P., Fuller, N., Gruner, S. M. & Parsegian, V. A. 1990 Membrane curvature, lipid segregation, and structural transitions for phospholipids under dual-solvent stress. *Biochemistry* **29**, 76–87.

Rand, R. P. & Parsegian, V. A. 1989 Hydration forces between phospholipid bilayers. *Biochim. Biophys. Acta* **988**, 351–376.

Sadoc, J. F. & Charvolin, J. 1986 Frustration in bilayers and topologies of liquid crystals of amphiphilic molecules. *J. Phys., Paris* **47**, 683–691.

Sadoc, J. F. & Charvolin, J. 1989 Infinite periodic minimal surfaces and their crystallography in the hyperbolic plane. *Acta Crystallogr.* A **45**, 10–20.

Schoen, A. H. 1970 Infinite periodic minimal surfaces without self-intersections. *NASA Tech. Note* TD-5541.

Schwarz, H. A. 1865 *Monatsberichte der Koniglichen Akademie der Wissenschaften zu Berlin*, Jahrgang 1865, pp. 149–153.

Scriven, L. E. 1976 Equilibrium bicontinuous structure. *Nature, Lond.* **263**, 123–125.

PHILOSOPHICAL TRANSACTIONS OF THE ROYAL SOCIETY A MATHEMATICAL, PHYSICAL & ENGINEERING SCIENCES

Scriven, L. E. 1977 Equilibrium bicontinuous structures. In *Micellization, solubilization and microemulsions*, vol. 2 (ed, K. L. Mittal), pp. 877–893. New York: Plenum Press.

Seddon, J. M. 1990*a* Structure of the inverted hexagonal (H_{II}) phase, and non-lamellar transitions of lipids. *Biochim. Biophys. Acta* **1031**, 1–69.

Seddon, J. M. 1990*b* An inverse face-centred cubic phase formed by diacylglycerol-phosphatidylcholine mixtures. *Biochemistry* **29**, 7997–8002.

Seddon, J. M. & Bartle, E. A. 1992 Inverse micellar cubic phases of lipids. In *The structure and conformation of amphiphilic membranes* (ed. R. Lipowsky, D. Richter & K. Kremer), pp. 257–261. Berlin: Springer-Verlag.

Seddon, J. M., Cevc, G., Kaye, R. D. & Marsh, D. 1984 X-ray diffraction study of the polymorphism of hydrated diacyl and dialkyl phosphatidylethanolamines. *Biochemistry* **23**, 2634–2644.

Seddon, J. M., Hogan, J. L., Warrender, N. A. & Pebay-Peyroula, E. 1990*a* Structural studies of phospholipid cubic phases. *Progr. Colloid Polym. Sci.* **81**, 189–197.

Seddon, J. M., Bartle, E. A. & Mingins, J. 1990*b* Inverse cubic liquid-crystalline phases of phospholipids and related lyotropic systems. *J. Phys. Condensed Matter* **2**, 285–290.

Shipley, G. 1973 Recent X-ray diffraction studies of biological membranes and membrane components. In *Biological membranes*, vol. 2 (ed. D. Chapman & D. F. H. Wallach), pp. 1–89. London: Academic Press.

Small, D. M., 1986 *Handbook of lipid research*, vol. 4. New York: Plenum Press.

Ström, P. & Anderson, D. M. 1992 The cubic phase region in the system didodecyl methylammonium bromide-water-styrene. *Langmuir* **8**, 691–709.

Szleifer, I., Kramer, D., Ben-Shaul, A., Gelbart, W. M. & Safran, S. A. 1990*a* Molecular theory of curvature elasticity in surfactant films. *J. chem. Phys.* **92**, 6800–6817.

Szleifer, I., Ben-Shaul, A. & Gelbart, W. M. 1990*b* Chain packing statistics and thermodynamics of amphiphile monolayers. *J. phys. Chem.* **94**, 5081–5089.

Tardieu, A. & Luzzati, V. 1970 Polymorphism of lipids. A novel cubic phase: a cage-like network of rods with enclosed spherical micelles. *Biochim. Biophys. Acta* **219**, 11–17.

Tate, M. W., Eikenberry, E. F., Turner, D. C., Shyamsunder, E. & Gruner, S. M. 1991 Nonbilayer phases of membrane lipids. *Chem. Phys. Lipids* **57**, 147–164.

Templer, R. H., Madan, K. H., Warrender, N. A,. & Seddon, J. M. 1992*a* Swollen lyotropic cubic phases in fully hydrated mixtures of monoolein, dioleoylphosphatidylcholine and dioleoylphosphatidylethanolamine. In *The structure and conformation of amphiphilic membranes* (ed. R. Lipowsky, D. Richter & K. Kremer), pp. 262–265. Berlin: Springer-Verlag.

Templer, R. H., Warrender, N. A., Meadows, R. & Seddon, J. M. 1992*b* Epitaxial relationships between adjacent phases in hydrated monoolein. In *The structure and conformation of amphiphilic membranes* (ed. R. Lipowsky, D. Richter & K. Kremer), pp. 230–233. Berlin: Springer-Verlag.

Terrones, H. & Mackay, A. L. 1992 The geometry of hypothetical curved graphite structures. *Carbon* **8**, 1251–1260.

Tiddy, G. J. T. 1980 Surfactant-water liquid crystal phases. *Phys. Rep.* **57**, 1–46.

Turner, D. C. & Gruner, S. M. 1992 X-Ray diffraction reconstruction of the inverted hexagonal (H_{II}) phase in lipid-water systems. *Biochemistry* **31**, 1340–1355.

Vargas, R., Mariani, P., Gulik, A. & Luzzati, V. 1992 The cubic phases of lipid-containing systems. The structure of phase Q^{223} (space group Pm3n): an X-ray scattering study. *J. molec. Biol.* **225**, 137–145.

PHILOSOPHICAL TRANSACTIONS OF THE ROYAL SOCIETY A MATHEMATICAL, PHYSICAL & ENGINEERING SCIENCES